丙第256号証の1

GEOPHYSICAL RESEARCH LETTERS, VOL. 39, L09306, doi:10.1029/2012GL051491, 2012

Unusual shallow normal-faulting earthquake sequence in compressional northeast Japan activated after the 2011 off the Pacific coast of Tohoku earthquake

Kazutoshi Imanishi,[1] Ryosuke Ando,[1] and Yasuto Kuwahara[1]

Received 24 February 2012; revised 2 April 2012; accepted 3 April 2012; published 5 May 2012.

[1] After the occurrence of the 2011 M_w 9.0 off the Pacific coast of Tohoku earthquake, an unusual shallow normal-faulting earthquake sequence occurred near the Pacific coast at the Ibaraki-Fukushima prefectural border. We have investigated why normal-faulting earthquakes were activated in northeast (NE) Japan, which is otherwise characterized by E–W compression. We computed the stress changes associated with the mainshock on the basis of a finite fault slip model, which showed that the amount of additional E–W tensional stresses in the study area was up to 1 MPa, which might be too small to generate normal-faulting earthquakes in the pre-shock compressional stress regime. We thus determined focal mechanisms of microearthquakes that occurred in the area before the mainshock, which indicated that the pre-shock stress field in the area showed a normal-faulting stress regime in contrast to the overall reverse-faulting regime in NE Japan. We concluded that the 2011 Tohoku earthquake triggered the normal-faulting earthquake sequence in a limited area in combination with a locally formed pre-shock normal-faulting stress regime. We also explored possible mechanisms for localization of a normal-faulting stress field at the Ibaraki-Fukushima prefectural border. **Citation:** Imanishi, K., R. Ando, and Y. Kuwahara (2012), Unusual shallow normal-faulting earthquake sequence in compressional northeast Japan activated after the 2011 off the Pacific coast of Tohoku earthquake, *Geophys. Res. Lett.*, *39*, L09306, doi:10.1029/2012GL051491.

1. Introduction

[2] The M_w 9.0 off the Pacific coast of Tohoku earthquake (hereafter referred to as "Tohoku earthquake") occurred on March 11, 2011 at 14:46 JST in the western Pacific Ocean, where the Pacific plate is subducting beneath northern Honshu at a rate of about 9 cm/yr (Figure 1a). This earthquake ruptured a 450 km-long in the NNE–SSW direction and 200-km-wide zone; it generated a large tsunami and caused great damage and loss of life in coastal areas. Inversion analyses of seismic, geodetic, and tsunami data suggest that coseismic slip exceeded 30 m over a wide area [e.g., *Fujii et al.*, 2011; *Loveless and Meade*, 2011; *Yoshida et al.*, 2011]. *Ide et al.* [2011] suggested a reversal of the stress state in the area of high slip due to a dynamic overshoot beyond zero shear stress there, as implied by the occurrence of normal-faulting aftershocks on the plate interface. The occurrence of this gigantic earthquake also influenced the tectonic stress fields throughout Japan, particularly in northeast Japan. For example, microearthquakes became active in volcanic regions, and several magnitude six or larger earthquakes occurred inland and off the coast in the Japan Sea [*Hirose et al.*, 2011].

[3] Among the triggered earthquakes, a particularly unusual event was a shallow normal-faulting earthquake sequence that occurred near the Pacific coast on the Ibaraki-Fukushima prefectural border, where background seismicity was low before the 2011 Tohoku earthquake (Figure 1). The sequence was characterized by swarm-like activity and contained an M_j7.0 earthquake on April 11 together with 24 moderate-magnitude earthquakes ($5.0 \leq M_j \leq 6.4$) as of 31 December 2011. Here, M_j is a magnitude determined by the Japan Meteorological Agency (JMA) [*Japan Meteorological Agency*, 2004]. The JMA earthquake catalogue defined the rupture zone as 80 km-long along strike; most of the events occurred at depths shallower than 15 km. The focal mechanisms of these earthquakes were of normal-faulting type with roughly E–W or NW–SE extension directions (Figure 1b). This area has been previously shown to contain active strike-slip- and normal-faulting faults; these are the Itozawa and Yunotake faults, respectively, and are indicated in Figure 1a [*Research Group for Active Faults of Japan*, 1991]. Field surveys reveal that both faults were ruptured during the M_j7.0 earthquake and that their surface ruptures were made up of normal fault scarps with offsets of up to 2 m [e.g., *Otsubo et al.*, 2012]. This extensional feature revealed by the normal-fault earthquakes is inconsistent with the present-day overall stress field in northeast Japan, which is characterized by a reverse-faulting regime with E–W compression [*Zoback*, 1992; *Kubo et al.*, 2002; *Townend and Zoback*, 2006]. In fact, as illustrated in Figure 1a, the E–W compressional feature is indicated by the reverse-faulting earthquakes approximately 70 km west of the Ibaraki-Fukushima prefectural border. The E–W compression is also supported by the presence of folds and reverse faults with strikes subparallel to the N–S direction [*Research Group for Active Faults of Japan*, 1991].

[4] *Kato et al.* [2011] inferred that the stress field of the present study area abruptly changed from horizontal compression to extension because trench-normal compressive stress within the overlying plate was reduced after the Tohoku earthquake. Although such a drastic change in stress state could occur in places close to the high-slip patch [*Hasegawa et al.*, 2011; *Ide et al.*, 2011], it is unclear why

[1]Geological Survey of Japan, Tsukuba, Japan.

Corresponding author: K. Imanishi, Geological Survey of Japan, AIST Tsukuba Central 7, 1-1-1 Higashi, Tsukuba, Ibaraki 305–8567, Japan. (imani@ni.aist.go.jp)

0094-8276/12/2012GL051491

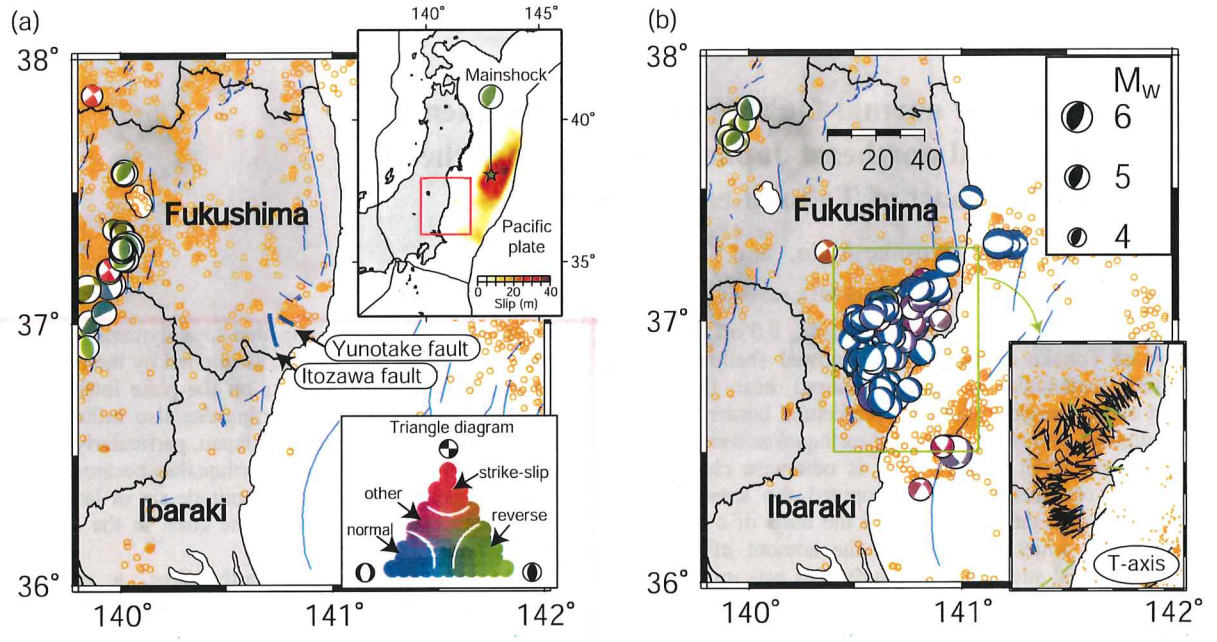

Figure 1. Spatial distribution of NIED F-net moment tensor solutions shallower than 15 km (a) before the 2011 Tohoku earthquake (January 1, 2000–March 10, 2011) and (b) after the earthquake (March 11–December 31, 2011). Best double couple solutions with variance reduction of larger than 70 are projected onto the lower hemisphere using the equal-area projection. Different colors are used to differentiate reverse (green), strike-slip (red), and normal (blue) faulting mechanisms; the triangle diagram with color scales is shown in Figure 1a. Orange circles show seismic activity shallower than 15 km based on the JMA catalogue. Active faults are represented by blue lines. Inset in Figure 1a shows the plate tectonic setting and slip distribution of the 2011 Tohoku earthquake [*Yoshida et al.*, 2011]. Inset in Figure 1b shows the azimuthal distribution of *T*-axes of earthquake focal mechanisms before (green) and after (black) the Tohoku earthquake, where focal mechanisms before the Tohoku earthquake are shown in Figure 3.

such a mechanism should have operated in the case of this study area, which is far from the plate boundary and the high-slip patch.

[5] In this study, we first computed stress changes associated with the mainshock on the basis of a finite fault slip model, which shows that the induced stresses alone could not have triggered this sequence if the area was presently subject to a reverse-faulting stress regime. We then determined the pre-shock stress field of the Ibaraki-Fukushima prefectural border using the focal mechanisms of microearthquakes that occurred before the 2011 Tohoku earthquake; this reveals that the area originally represented a normal-faulting regime. As results, we conclude that the 2011 Tohoku earthquake triggered the normal-faulting earthquake sequence in a limited area in combination with a local pre-shock normal-faulting stress regime. Based on these results, we introduce a model for localizing a normal-faulting stress field in the specific region of northeast Japan.

2. Stress Transferred by the 2011 Tohoku Earthquake

[6] In order to quantitatively investigate whether normal-faulting type earthquakes were activated by the 2011 Tohoku earthquake, we computed stress changes due to the mainshock. Calculations were made in an elastic half-space following *Okada* [1992]; a shear modulus of 32 GPa and Poisson's ratio of 0.25 were assumed. We used the variable slip model derived from inversion of regional strong motion waveform data [*Yoshida et al.*, 2011] (inset of Figure 1a), in which the average rake vector 82.5°, the peak slip reaches 38 m, and the total seismic moment is 3.4×10^{22} Nm (M_w = 9.0). This model is generally consistent with other published slip models based on teleseismic [e.g., *Ide et al.*, 2011], geodetic [e.g., *Loveless and Meade*, 2011], and tsunami data [e.g., *Fujii et al.*, 2011] where the high slip region is located near the trench. Figure 2a shows the orientations of the induced principal stresses at a depth of 8 km. The results show that the stress changes associated with the 2011 Tohoku earthquake produced normal- and strike-slip-faulting stress fields over a wide region, including the target area. The minimum principal stress axes trend approximately E–W. These results are not unexpected because tensional stress is caused by the overriding plate being pulled eastward. Figure 2b shows a map view of the deviatoric minimum stress (hereafter referred to as "extensional stress") at a depth of 8 km; it indicates that an extensional stress of up to 1 MPa was induced at the target area. Although the induced extensional stress clearly favors the activation of normal-fault earthquakes [*Hiratsuka and Sato*, 2011; *Toda et al.*, 2011], a key question is whether the induced stress could overcome a pre-existing compressional reverse stress state. Much of the data obtained from deep boreholes suggest that an appropriate reference stress state for an intraplate continental upper crust is governed by optimally oriented, cohesionless faults under the conditions of hydrostatic pore pressure and Byerlees's friction law [e.g., *Townend*, 2006]. If so, a depth-averaged differential stress of the upper crust could be

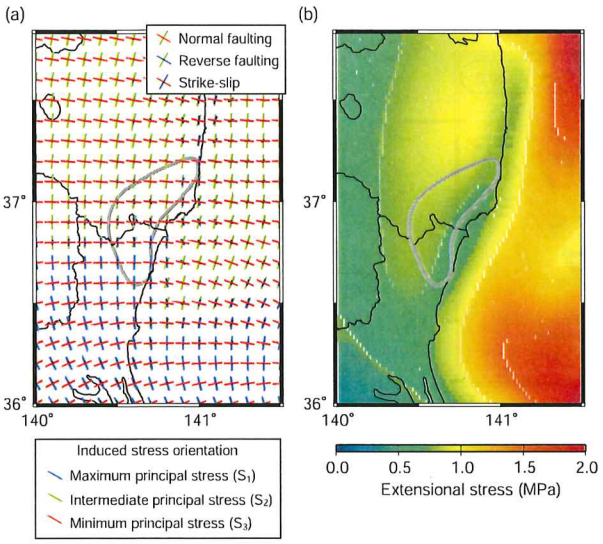

Figure 2. Stress tensor changes at a depth of 8 km associated with the 2011 Tohoku earthquake. (a) Orientations of induced principal stresses, where the bar length is proportional to the projection of the stress orientation on the horizontal component (the bar corresponding to a vertical direction would have zero length). (b) Map view of extensional stress at a depth of 8 km. The gray curve roughly represents the area of the normal-faulting earthquake sequence.

comparable to 150 MPa in a reverse fault stress regime, which is high compared to the induced extensional stress. *Seno* [1999] synthesized the principal stresses of Japanese islands based on ridge push and slab pull forces of the subducting oceanic plate and force variations across the arc due to crust/plate structural variation. The estimated differential stress in Tohoku area is 32–50 MPa, which is also high compared to our estimate of the induced extensional stress. We infer that the stress changes alone could not trigger this sequence if this area was presently subject to a reverse-faulting stress regime.

3. Stress Field Along the Ibaraki-Fukushima Prefectural Border Before the 2011 Tohoku Earthquake

[7] For earthquakes that occurred in the target area before the 2011 Tohoku earthquake, only one first-motion focal mechanism solution exists in the JMA catalogue, and none are in the F-net moment tensor solution catalogue (http://www.fnet.bosai.go.jp/) by National Research Institute for Earth Science and Disaster Prevention (NIED). This is because earthquakes that occurred in the target area were small in magnitude, so we determined the focal mechanism solutions of microearthquakes in and around the target area using the absolute body wave amplitude as well as the *P*-wave polarity. The same approach was used in our previous studies [e.g., *Imanishi et al.*, 2011] and shown to be effective for small earthquakes, even if the number of *P*-wave polarities is insufficient.

[8] We analyzed earthquakes occurring before the 2011 Tohoku event with magnitude (M_j) larger than 1.5, focal depths less than 20 km, and at least 8 *P*-wave polarities. The data for this analysis came from the regional high-sensitivity seismic stations. In total, we obtained 26 focal mechanisms of earthquakes that occurred between 2003 and 2010. Figure 3a shows the spatial distributions of the focal mechanisms in four different depth ranges together with the seismicity of the normal-faulting earthquake sequence as a reference. In every depth section, earthquakes located outside and at the western margin of the sequence (marked "a" in Figure 3a) are characterized by reverse-faulting, strike-slip faulting, or a mixture of both components, and the *P*-axis trended in the E–W direction approximately. This feature is consistent with the general tectonic trend in northeast Japan as described above (see also Figure 1a). In contrast, earthquakes located within the source region of the normal-faulting earthquake sequence (marked "b" in Figure 3a) exhibit normal-faulting, strike-slip faulting, or a mixture of both. The spatial distribution of the *T*-axis azimuth is similar to that after the Tohoku earthquake; namely a gradual clockwise rotation of the *T*-axis from south to north (Figure 1b). This extensional feature is clearly different from that of the general tectonic trend in northeast Japan. In the paper of *Kato et al.* [2011], only four events all with reverse-faulting components are shown to represent the stress state in the source region of the normal-faulting earthquake sequence before the 2011 Tohoku event. The focal mechanisms of the same events were determined in this study and certainly represent reverse-faulting with the *P*-axis oriented in the E–W direction (four events marked with "a" at the deepest depth section in Figure 3a). In contrast to *Kato et al.* [2011], we consider these earthquakes to represent stress fields outside the source region of the sequence because they were located near the western margin of the normal-faulting earthquake sequence at depths deeper than 16 km.

[9] Using the focal mechanism solutions determined in the present study, we have calculated the stress field in the target area before the 2011 Tohoku earthquake by applying the inversion method of *Michael* [1984]. The actual procedure we used was the same as that by *Imanishi et al.* [2011]. Here we only use the focal mechanisms marked with "b" in Figure 3a. The results of the stress tensor inversion are shown in Figure 3b. The 95% confidence regions of the stress orientations are relatively large because of the small number of mechanisms available. However, in spite of these large uncertainties, the stress tensor inversion reveals that the target area was characterized by a normal-faulting stress regime with the minimum principal stress S_3 oriented in the NW–SE direction subhorizontally. It should be emphasized that the pre-Tohoku earthquake stress field in the target area was a normal-faulting regime, which is an important factor in terms of the activation of the normal-faulting earthquake sequence. We conclude that the stress changes associated with the 2011 Tohoku earthquake could have triggered the normal-faulting earthquake sequence at the Ibaraki-Fukushima prefectural border in combination with the estimated pre-shock normal-faulting stress regime.

4. Explanatory Model of a Normal-Faulting Stress Field in the Study Area

[10] The stress tensor inversion reveals that the pre-Tohoku earthquake stress field at the Ibaraki-Fukushima prefectural border was originally under a normal-faulting stress regime. Generally such an extensional regime is known

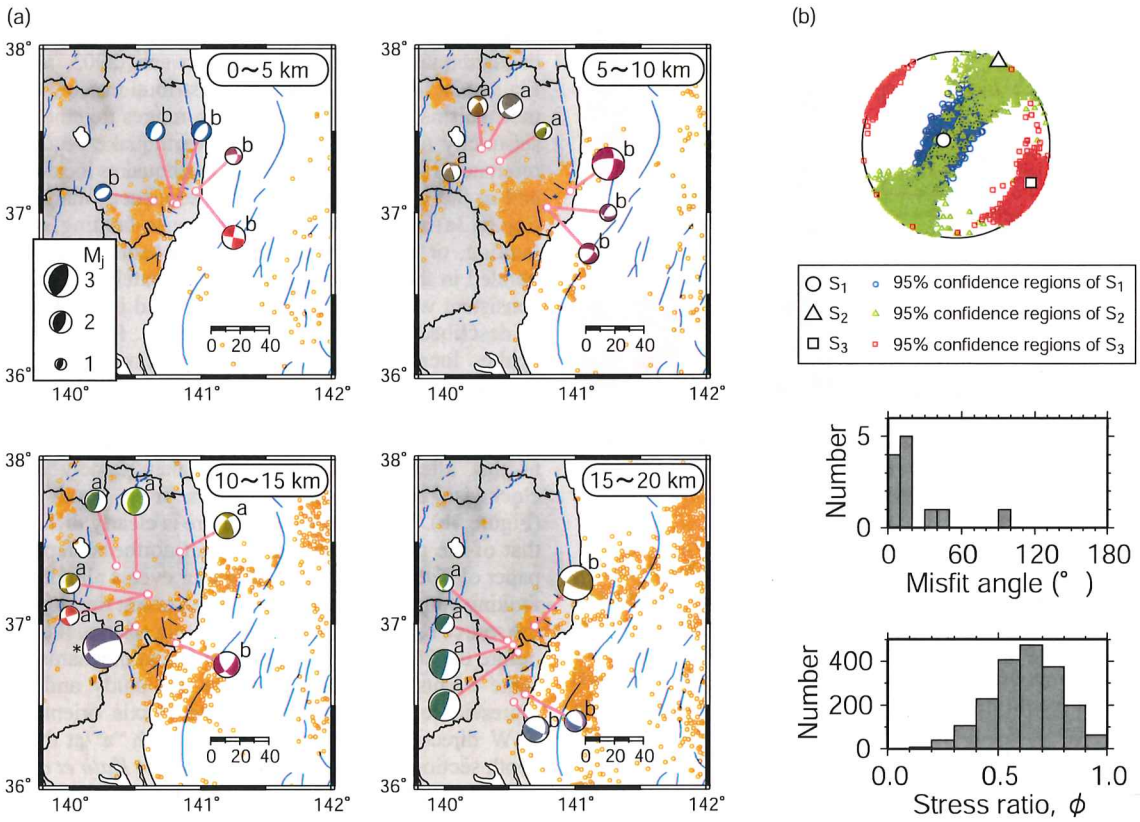

Figure 3. (a) Focal mechanism solutions of microearthquakes determined in the present study that occurred before the 2011 Tohoku earthquake (lower hemisphere, equal-area projection). The same triangle diagram as that of Figure 1 is used to differentiate faulting types. A mechanism marked with asterisk is also listed in the JMA catalogue; this is almost the same as that determined by JMA. The alphabetical letters "a" or "b" denote events which are outside or within the source area of the normal-faulting earthquake sequence. (b) Stress tensor inversion result. (top) Principal stress axes with their 95% confidence regions plotted on lower hemisphere stereonets. (middle) Misfit angle for the data with respect to the best stress tensor determined by the stress tensor inversion. Here, the misfit angle represents the angle between the tangential traction predicted by the best solution and the observed slip direction on each plane determined from the focal mechanism. (bottom) Histogram of stress ratio $\phi = (S_2 - S_3)/(S_1 - S_3)$ that belongs to the 95% confidence region.

to exist in high mountain belts such as the Tibetan plateau and high Andes [e.g., *Zoback*, 1992], where the mountains relief and crustal roots (negative Bouguer anomaly) produce extensional stresses. However, the same mechanism cannot explain the normal-faulting stress field in the study area because the altitude (which averages about 500 m above mean sea level) is much lower than those mountain belts. Furthermore, the Bouguer anomaly in the area is positive [*Makino et al.*, 1995], which is opposite to the situation in high mountain belts. An increase in vertical stress may have produced a component of normal faulting in the area, although it was limited to the near-surface region. Instead of these possible mechanisms, we here present another mechanism that can possibly form a normal-faulting stress field over a shallow seismogenic zone at the Ibaraki-Fukushima prefectural border, based on the seismicity distribution pattern and spatial extent of the normal-faulting earthquake sequence.

[11] Figure 4a shows trench-perpendicular cross-sections of aftershocks created by the JMA catalogue. Although the hypocentral accuracy of the JMA catalogue decreases for the offshore due to the geometry of the land-based seismic network, the aftershock distribution clearly delineates low-angle landward-dipping alignments for every cross-section corresponding to the plate boundary. We also observe low-angle seaward-dipping alignments, especially for cross-sections E–E′, which is located above the plate boundary. Seismic activity in the alignment commenced after the 2011 Tohoku earthquake. The upward extension of the alignment in cross-section E–E′ connects with the area of the normal-faulting earthquake sequence, which was also identified by the background seismicity.

[12] The above observations favor the hypothesis that the alignment represents a weak zone compared to the surrounding region and that a displacement along the alignment (hereafter referred to as a "branching fault") occurred during or shortly after the mainshock. We represent the geometry of the branching fault as a 60 km × 70 km fault with a strike of 20° and dip of 20° (blue square and line, respectively, in Figure 4a) based on the seismicity distribution pattern and spatial extent of the normal-faulting earthquake sequence. Analysis of the Coulomb stress change (ΔCFF) indicates that the low-angle interplate earthquake promote normal-faulting slip along the branching fault and inhibited reverse-faulting

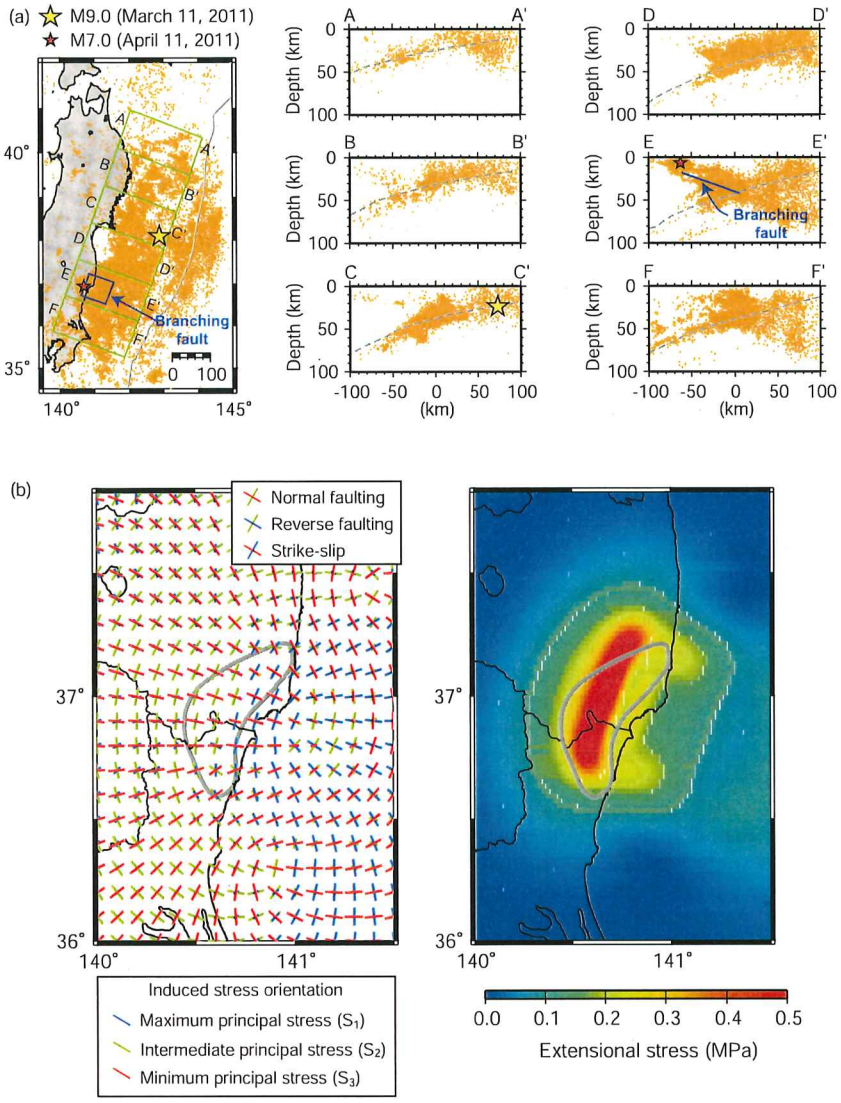

Figure 4. (a) Vertical cross-sections of aftershocks (March 11–December 31, 2011) on the basis of the JMA catalogue (orange circles). Aftershocks with a magnitude greater than 2 are plotted. The locations of each section are shown by green rectangles on the map. The blue square on the map and line in cross-section E–E′ define the geometry of a branching normal fault. Gray broken lines represent the upper boundary of the subducted Pacific plate [*Kita et al.*, 2010; *Nakajima and Hasegawa*, 2006]. Yellow and red stars correspond to the location of the 2011 Tohoku earthquake and the M_j7.0 normal-faulting earthquake on April 11, 2011. (b) Stress tensor changes at a depth of 8 km associated with the normal-faulting slip along the branching fault. (left) Orientations of induced principal stresses. (right) Map view of extensional stress.

slip, so the rake angle is assumed to be −90°. We calculate the stress changes due to slip on the branching fault using the same approach as in section 2. Here, we assume 1 m of slip on the fault for the sake of convenience in the absence of information regarding the amount of slip. Figure 4b shows the computed stress tensor changes at a depth of 8 km. For the Ibaraki-Fukushima prefectural border, the pattern of the computed stress field represents a normal-faulting regime, which is consistent with the observational evidence. The magnitude of the computed extensional stress is also shown in Figure 4b, where the extensional stress is localized to the Ibaraki-Fukushima prefectural border due to stress concentration. This model explains the gradual clockwise rotation of the tensional axis from south to north, which was observed both before and after the Tohoku earthquake (see Figure 1b).

[13] Figures 2 and 4b suggest that interplate earthquakes as well as normal fault displacements along the branching fault form normal-faulting stress fields at shallow depths over a wide area. We infer that normal-faulting stress fields will be more or less cancelled by the E–W compressional stress due to tectonic loading and that most regions will return to the regional stress field with time. However, it will take much longer time for the stress concentration region to return to the regional stress field. If the induced normal-faulting stress and tectonic loading stress do not completely cancel each other, normal-fault stresses at shallow depths accumulate over

several earthquake cycles. This scenario may explain why a specific region of northeast Japan is characterized by a normal-faulting stress field.

[14] The ΔCFF analysis implies that slip on the branching fault was closely linked with that on the interplate earthquake. Similar normal-faulting also occurred after the 2010 M_w 8.8 Maule megathrust earthquake in south-central Chile [*Farías et al.*, 2011]. In the present case, there is no direct evidence to suggest normal fault slip along the branching fault during the mainshock or large aftershocks, although earthquakes around the seaward-dipping alignment generally have normal-faulting mechanisms (NIED F-net moment tensor solutions). However, we cannot rule out branching normal fault failure during mainshock faulting because the source inversion generally retrieves the slip distribution by assuming a fault geometry and a sense of slip a priori. Detailed analysis of the entire rupture process of the mainshock will be part of future work.

5. Discussions and Conclusion

[15] We have demonstrated that stress changes caused by the 2011 Tohoku earthquake combined with a pre-shock normal-faulting stress regime could have triggered the normal-faulting earthquake sequence at the Ibaraki-Fukushima prefectural border. This contradicts the interpretation of *Kato et al.* [2011], who argued that a reversal of stress state occurred as a result of the Tohoku earthquake. By inverting focal mechanism data before and after the 2011 Tohoku earthquake, *Yoshida et al.* [2012] inferred that stress regime drastically changed over inland areas of northern Tohoku together with the present study area. However, more consideration needs to be given to ensure that spatial variations in stress can be ruled out, because pre- and post-earthquake stress estimates are not always derived from earthquakes that occurred at the same location in space as shown in Figure 2 of *Yoshida et al.* [2012]. One of the main contributions of this paper is the demonstration that unless the stress fields before the Tohoku earthquake is carefully examined some stress states after the Tohoku earthquake will be misinterpreted as such temporal changes in stress regime.

[16] If we look at other coastal areas in convergent tectonic settings, several observations exist that suggest the same extensional feature as the Ibaraki-Fukushima prefectural border. For example, *Yamamoto et al.* [2004] conducted in-situ stress measurements on the Pacific coast between 39°N and 40.5°N (the Sanriku area) and found that the area is characterized by tensional stresses trending N–S or NE–SW. Neogene deformation in the northern Chilean forearc (21°–25°S) is known to be dominated by structures indicating extension in the direction of plate convergence, where numerous normal faults and open cracks occur both onshore and offshore [e.g., *Loveless et al.*, 2010]. In the Hikurangi subduction margin along the Raukumara Peninsula of New Zealand (37.5°–39.5°S), microearthquakes with a normal-faulting component occur in the upper crust of the overlying plate in conjunction with the presence of Neogene extensional structures [e.g., *Reyners and McGinty*, 1999].

[17] We have explored a possible scenario, the branching normal fault hypothesis, to explain the localization of a normal-faulting stress field at the Ibaraki-Fukushima prefectural border and account for the features of the observed *T*-axis distribution. In the Sanriku area, we can also identify earthquake clusters above the plate boundary in the background and post-mainshock seismicity (see cross-section B–B′ in Figure 4a), although the post-shock seismicity is not as active as that along cross-section E–E′. The extensional stress field formed along the coast of the Sanriku area may therefore be explained by a stress concentration associated with past repeated normal-fault slips along a branching fault. A curvature effect of the subduction plate interface [e.g., *Hashimoto and Matsu'ura*, 2006] also provides a mechanism for producing extensional stresses. Furthermore, the effect of upper plate bending is a candidate explanation since convex upward bending can produce large tension locally for the shallower side of the plate that exceeds horizontal compression due to subduction [e.g., *Turcotte and Schubert*, 2002]. The seaward-dipping alignment of the upper plate seismicity may imply such bending has maximum curvature around the currently targeted coastal area. Other models have been proposed to explain the presence of extensional structures, including long-term extension and uplift caused by subduction erosion in both northern Chile and the Raukumara Peninsula of New Zealand [*Reyners and McGinty*, 1999; *von Huene et al.*, 1999] and strains associated with interseismic locking on the plate boundary in northern Chile [*Loveless et al.*, 2010]. The distance scales over which extensional stress actually appears are less than several hundred kilometers, while some of the mechanisms described above would affect areas of greater dimensions. It is important to examine further which model or combination of models is better applicable to the north Chile and Raukumara Peninsula cases as well as the current target of the Pacific subduction zone.

[18] **Acknowledgments.** We are grateful to JMA for the earthquake catalogue and NIED for F-net moment tensor solutions. Seismograph stations used in this study include permanent stations operated by NIED (Hi-net), JMA, and Tohoku University. Comments by J. Townend, M. Tingay and an anonymous reviewer were helpful in improving the paper. Y. Yoshida kindly provided us his finite fault source model. We modified a program coded by S. Ide to estimate the focal mechanism solutions. "Slick Package" (http://earthquake.usgs.gov/research/software/) was used in the stress tensor inversion. We thank Y. Okada for the use of his code in our stress field investigation. Figures were generated using the Generic Mapping Tool [*Wessel and Smith*, 1998].

[19] The Editor thanks John Townend and an anonymous reviewer for assisting with the evaluation of the paper.

References

Farías, M., D. Comte, S. Roecker, D. Carrizo, and M. Pardo (2011), Crustal extensional faulting triggered by the 2010 Chilean earthquake: The Pichilemu Seismic Sequence, *Tectonics*, *30*, TC6010, doi:10.1029/2011TC002888.

Fujii, Y., K. Satake, S. Sakai, M. Shinohara, and T. Kanazawa (2011), Tsunami source of the 2011 off the Pacific coast of Tohoku earthquake, *Earth Planets Space*, *63*, 815–820, doi:10.5047/eps.2011.06.010.

Hasegawa, A., K. Yoshida, and T. Hasegawa (2011), Nearly complete stress drop in the 2011 M_w 9.0 off the Pacific coast of Tohoku earthquake, *Earth Planets Space*, *63*, 703–707, doi:10.5047/eps.2011.06.007.

Hashimoto, C., and M. Matsu'ura (2006), 3-D simulation of tectonic loading at convergent plate boundary zones: Internal stress fields in northeast Japan, *Pure Appl. Geophys.*, *163*, 1803–1817, doi:10.1007/s00024-006-0098-y.

Hiratsuka, S., and T. Sato (2011), Alteration of stress field brought about by the occurrence of the 2011 off the Pacific coast of Tohoku earthquake (M_w 9.0), *Earth Planets Space*, *63*, 681–685, doi:10.5047/eps.2011.05.013.

Hirose, F., K. Miyaoka, N. Hayashimoto, T. Yamazaki, and M. Nakamura (2011), Outline of the 2011 off the Pacific coast of Tohoku earthquake (M_w 9.0)—Seismicity: Foreshocks, mainshock, aftershocks, and induced activity—, *Earth Planets Space*, *63*, 513–518, doi:10.5047/eps.2011.05.019.

Ide, S., A. Baltay, and G. C. Beroza (2011), Shallow dynamic overshoot and energetic deep rupture in the 2011 M_w 9.0 Tohoku-Oki earthquake, *Science, 332*, 1426–1429, doi:10.1126/science.1207020.

Imanishi, K., Y. Kuwahara, T. Takeda, T. Mizuno, H. Ito, K. Ito, H. Wada, and Y. Haryu (2011), Depth-dependent stress field in and around the Atotsugawa fault, central Japan, deduced from microearthquake focal mechanisms: Evidence for localized aseismic deformation in the downward extension of the fault, *J. Geophys. Res.*, *116*, B01305, doi:10.1029/2010JB007900.

Japan Meteorological Agency (2004), *The Seismological and Volcanological Bulletin of Japan for January 2004*, Tokyo.

Kato, A., S. Sakai, and K. Obara (2011), A normal-faulting seismic sequence triggered by the 2011 off the Pacific coast of Tohoku earthquake: Wholesale stress regime changes in the upper plate, *Earth Planets Space*, *63*, 745–748, doi:10.5047/eps.2011.06.014.

Kita, S., T. Okada, A. Hasegawa, J. Nakajima, and T. Matsuzawa (2010), Anomalous deepening of a seismic belt in the upper-plane of the double seismic zone in the Pacific slab beneath the Hokkaido corner: Possible evidence for thermal shielding caused by subducted forearc crust materials, *Earth Planet. Sci. Lett.*, *290*, 415–426, doi:10.1016/j.epsl.2009.12.038.

Kubo, A., E. Fukuyama, H. Kawai, and K. Nonomura (2002), NIED seismic moment tensor catalogue for regional earthquakes around Japan: Quality test and application, *Tectonophysics*, *356*, 23–48, doi:10.1016/S0040-1951(02)00375-X.

Loveless, J. P., and B. J. Meade (2011), Spatial correlation of interseismic coupling and coseismic rupture extent of the 2011 M_W = 9.0 Tohoku-oki earthquake, *Geophys. Res. Lett.*, *38*, L17306, doi:10.1029/2011GL048561.

Loveless, J. P., R. W. Allmendinger, M. E. Pritchard, and G. González (2010), Normal and reverse faulting driven by the subduction zone earthquake cycle in the northern Chilean fore arc, *Tectonics*, *29*, TC2001, doi:10.1029/2009TC002465.

Makino, M., et al. (1995), Gravity map of Abukuma district (Bouguer Anomalies), scale 1:200,000, *Gravity Map Ser. 6*, Geol. Surv. Jpn., Tsukuba.

Michael, A. J. (1984), Determination of stress from slip data: Faults and folds, *J. Geophys. Res.*, *89*(B13), 11,517–11,526, doi:10.1029/JB089iB13p11517.

Nakajima, J., and A. Hasegawa (2006), Anomalous low-velocity zone and linear alignment of seismicity along it in the subducted Pacific slab beneath Kanto, Japan: Reactivation of subducted fracture zone?, *Geophys. Res. Lett.*, *33*, L16309, doi:10.1029/2006GL026773.

Okada, Y. (1992), Internal deformation due to shear and tensile faults in a half-space, *Bull. Seismol. Soc. Am.*, *82*, 1018–1040.

Otsubo, M., N. Shigematsu, M. Takahashi, T. Azuma, K. Imanishi, and R. Ando (2012), Slickenlines on fault scarps caused by an earthquake in Iwaki-city (Fukushima Prefecture, Japan) on 11th of April, 2011, *J. Geol. Soc. Jpn.*, *118*, III–IV.

Research Group for Active Faults of Japan (1991), *Active Faults of Japan* [in Japanese], Univ. of Tokyo Press, Tokyo.

Reyners, M., and P. McGinty (1999), Shallow subduction tectonics in the Raukumara Peninsula, New Zealand, as illuminated by earthquake focal mechanisms, *J. Geophys. Res.*, *104*(B2), 3025–3034, doi:10.1029/1998JB900081.

Seno, T. (1999), Syntheses of the regional stress fields of the Japanese islands, *Isl. Arc*, *8*, 66–79, doi:10.1046/j.1440-1738.1999.00225.x.

Toda, S., J. Lin, and R. S. Stein (2011), Using the 2011 Mw9.0 off the Pacific coast of Tohoku earthquake to test the Coulomb stress triggering hypothesis and to calculate faults brought closer to failure, *Earth Planets Space*, *63*, 725–730, doi:10.5047/eps.2011.05.010.

Townend, J. (2006), What do faults feel? Observational constraints on the stresses acting on seismogenic faults, in *Earthquakes: Radiated Energy and the Physics of Earthquake Faulting*, *Geophys. Monogr. Ser.*, vol. 170, edited by R. Abercrombie et al., pp. 313–327, AGU, Washington, D. C., doi:10.1029/170GM31

Townend, J., and M. D. Zoback (2006), Stress, strain, and mountain building in central Japan, *J. Geophys. Res.*, *111*, B03411, doi:10.1029/2005JB003759.

Turcotte, D. L., and J. Schubert (2002), *Geodynamics*, 2nd ed., 456 pp., Cambridge Univ. Press, Cambridge, U. K.

von Huene, R., W. Weinrebe, and F. Heeren (1999), Subduction erosion along the north Chile margin, *J. Geodyn.*, *27*, 345–358, doi:10.1016/S0264-3707(98)00002-7.

Wessel, P., and W. H. F. Smith (1998), New, improved version of the Generic Mapping Tools released, *Eos Trans. AGU*, *79*, 579, doi:10.1029/98EO00426.

Yamamoto, K., N. Sato, and Y. Yabe (2004), Driving force of the intraplate crust as inferred from the stresses measured in the eastern part of Kitakami mountains, northeastern Honshu, Japan [in Japanese with English abstract], *J. Seismol. Soc. Jpn.*, *56*, 511–527.

Yoshida, K., A. Hasegawa, T. Okada, T. Iinuma, Y. Ito, and Y. Asano (2012), Stress before and after the 2011 great Tohoku-oki earthquake and induced earthquakes in inland areas of eastern Japan, *Geophys. Res. Lett.*, *39*, L03302, doi:10.1029/2011GL049729.

Yoshida, Y., H. Ueno, D. Muto, and S. Aoki (2011), Source process of the 2011 off the Pacific coast of Tohoku earthquake with the combination of teleseismic and strong motion data, *Earth Planets Space*, *63*, 565–569, doi:10.5047/eps.2011.05.011.

Zoback, M. L. (1992), First- and second-order patterns of stress in the lithosphere: The world stress map project, *J. Geophys. Res.*, *97*, 11,703–11,728, doi:10.1029/92JB00132.

【1頁】

GEOPHYSICAL RESEARCH LETTERS,VOL.39,L09806,doi:10.1029/2012GL051491,2012

2011 年東北地方太平洋沖地震の発生後に，圧縮応力場である東北日本で起きた，浅部の正断層型地震が続発するという稀な活動について

今西和俊，安藤亮輔，桑原保人

2012 年 2 月 24 日受付;2012 年 4 月 2 日訂正,2012 年 4 月 3 日受理,2012 年 5 月 5 日発表

2011 年東北地方太平洋沖地震（モーメントマグニチュード Mw9.0）の発生後に，茨城県・福島県境の太平洋海岸付近で，浅部の正断層型地震が続発するという稀な活動が起きた。筆者らは，東西圧縮が卓越している東北日本において，正断層型地震が活性化した要因を調査してきた。 有限断層すべりモデルを用いて本震による応力変化を計算した結果，調査地域における東西引張応力の増加量は 1MPa までであり，その数値は，元々圧縮応力場であった場所において，正断層型地震を作りだすにはあまりにも小さかったことが分かった。 そこで，本震前にこの地域で発生した微小地震の発震機構を求めたところ，東北日本において多い逆断層型ではなく，この地域における元々の応力場は正断層型であった。 これらのことから，2011 年東北地震によって，元々正断層応力場であった地域において，局所的に正断層地震活動が活発化したとの結論を得た。また，茨城県・福島県境において局所的に正断層応力場となりうるメカニズムについても調査した。

（略）